Timing of Examination Affects Reliability of ^{99m}Tc-Methoxyisobutylisonitrile SPECT in Distinguishing Neoplastic from Nonneoplastic Brain Hematomas

Fabio Minutoli, MD[1]; Filippo F. Angileri, MD, PhD[2]; Alfredo Conti, MD[2]; Astrid Herberg, MD[1]; Demetrio Aricò, MD[1]; Sara Baldari, MD[1]; Salvatore Cardali, MD[2]; Oreste de Divitiis, MD[2]; Antonino Germanò, MD[2]; and Sergio Baldari, MD[1]

[1]Department of Radiological Sciences, University of Messina, Messina, Italy; and [2]Department of Neurosciences, Psychiatry, and Anesthesiology, University of Messina, Messina, Italy

^{99m}Tc-Methoxyisobutylisonitrile (MIBI) SPECT has been reported to be 100% sensitive and specific in the early differential diagnosis between neoplastic and nonneoplastic intraparenchymal cerebral hemorrhage (ICH), because nonneoplastic ICH does not show ^{99m}Tc-MIBI accumulation on SPECT examinations performed within 48 h from the onset of clinical symptoms. The aims of this study were to investigate the behavior of nonneoplastic ICH on more delayed ^{99m}Tc-MIBI SPECT examinations and to determine how the timing of examination affects the reliability of ^{99m}Tc-MIBI SPECT in differentiating neoplastic from nonneoplastic ICH. **Methods:** We prospectively enrolled 32 patients with acute neurologic deterioration caused by nontraumatic ICH. Patients were randomly allocated to 4 groups of 8 patients each. Patients in the first, second, third, and fourth groups underwent ^{99m}Tc-MIBI SPECT 2, 5, 10, and 30 d, respectively, after the onset of clinical deterioration. Furthermore, patients in the first group underwent a second ^{99m}Tc-MIBI SPECT examination at 30 d. ^{99m}Tc-MIBI SPECT studies were visually and semiquantitatively evaluated. Patients were followed up to confirm the nonneoplastic etiology of the ICH. **Results:** Two of the 32 studied patients, 1 in the second and 1 in the fourth group, were excluded because the ICH turned out to be related to a neoplastic lesion. Visual analysis showed no ^{99m}Tc-MIBI uptake in any patient studied at 2 d, whereas increased radiotracer uptake was found in 1 (14%) of 7, 5 (62.5%) of 8, and 5 (71%) of 7 patients studied 5, 10, and 30 d, respectively, after clinical deterioration. Moreover, with the semiquantitative analysis, a statistically significant difference was found among ^{99m}Tc-MIBI indices in the 4 groups ($P = 0.0011$). All patients in group 1 showed a significant ^{99m}Tc-MIBI accumulation when studied at 30 d. **Conclusion:** Nonneoplastic ICH, showing no ^{99m}Tc-MIBI uptake within 2 d, can show ^{99m}Tc-MIBI accumulation on more delayed imaging. ^{99m}Tc-MIBI SPECT can clearly differentiate between neoplastic and nonneoplastic ICH only during the acute phase. Our findings suggest that examination be performed early after the onset of symptoms and certainly within 5 d.

Key Words: ^{99m}Tc-sestamibi; SPECT; intracranial hemorrhage; brain tumor; specificity

J Nucl Med 2005; 46:574–579

Distinguishing neoplastic from nonneoplastic intracerebral hematoma is a challenging problem because neoplasms can be hidden behind an intraparenchymal cerebral hemorrhage (ICH) (*1–4*) and some hemorrhagic nonneoplastic lesions may mimic neoplasms on standard neuroradiologic images (*5,6*).

In a recent paper (*7*), ^{99m}Tc-methoxyisobutylisonitrile (MIBI) SPECT was proposed as a useful tool in the early differential diagnosis of ICH. The differential diagnosis was based on the lack of radiotracer accumulation in nonneoplastic ICH. All cases of ICH in that study were evaluated within 48 h after the onset of clinical symptoms, and ^{99m}Tc-MIBI SPECT turned out to be strongly sensitive and specific.

Because the neuropathologic features of ICH are known to change significantly over time (*8–12*), the ^{99m}Tc-MIBI SPECT findings for nonneoplastic hemorrhage could be expected to change concurrently. Furthermore, because patients may come to clinical attention or undergo ^{99m}Tc-MIBI SPECT during the subacute stage of ICH, verification of the behavior of ^{99m}Tc-MIBI accumulation in nonneoplastic ICH on delayed SPECT examinations seems to be clinically relevant. Indeed, if, on delayed SPECT examinations, ^{99m}Tc-MIBI is taken up by both nonneoplastic and neoplastic ICH, these 2 entities become indistinguishable.

The aims of this study were to investigate the appearance of nonneoplastic ICH on early and delayed ^{99m}Tc-MIBI SPECT examinations and to determine how the timing of

Received Sep. 12, 2004; revision accepted Nov. 23, 2004.

For correspondence or reprints contact: Filippo F. Angileri, MD, PhD, Department of Neurosciences, Psychiatry, and Anesthesiology, University of Messina, Clinica Neurochirurgica, A.O.U. "Policlinico G. Martino," Via Consolare Valeria, 98100 Messina, Italy.

E-mail: fangileri@unime.it

the examination can affect the reliability of ^{99m}Tc-MIBI SPECT in differentiating neoplastic from nonneoplastic ICH.

MATERIALS AND METHODS

Patient Population

We prospectively enrolled 32 consecutive patients (Table 1) admitted to our hospital because of an acute neurologic deterioration caused by nontraumatic ICH. ICH was demonstrated by an emergency CT scan. Each patient had to meet all of the following inclusion criteria: a nontraumatic acute onset of clinical deterioration, ICH demonstrated by emergency CT, no known brain neoplasm, a single lesion evident on brain CT, no history of previous ICH, and no need for emergent craniotomy. Patients with pituitary, pure subarachnoid, or pure intraventricular hemorrhage were excluded.

After inclusion, patients were randomly allocated to 4 groups, each consisting of 8 patients. Patients in the first group underwent ^{99m}Tc-MIBI SPECT 2 d after the onset of clinical symptoms. Patients in the second, third, and fourth groups underwent ^{99m}Tc-MIBI SPECT 5, 10, and 30 d, respectively, after the onset. Furthermore, patients in the first group underwent a second ^{99m}Tc-MIBI SPECT examination 30 d after the onset.

All patients were followed up clinically and neuroradiologically (CT, MRI, and digital subtraction angiography) according to our standard diagnostic protocols to confirm the nonneoplastic etiology of the studied hematomas. Patients were followed up until a definitive diagnosis was obtained. Data were evaluated after follow-up of all patients had been completed.

The study was approved by our institutional review board, and informed consent was obtained from each patient.

^{99m}Tc-MIBI SPECT Protocol

Images were acquired on a dual-head γ-camera (Odyssey; Picker International), using a circular orbit and high-resolution collimators with a 128 × 128 matrix, a 360° rotation, a 3° step-and-shoot technique, and an acquisition time of 25 s per frame, 10 min after intravenous injection of 740 MBq (20 mCi) of ^{99m}Tc-MIBI. The data were processed using ramp-filtered backprojection and attenuation correction (correction factor, 0.110) with a low-pass filter. The data were displayed 2 pixels thick (4.6 mm) in transaxial, sagittal, and coronal slices, followed by orbitomeatal line reorientation of the reconstructed volume.

TABLE 1
Clinical Data and ^{99m}Tc-MIBI Uptake in 32 Consecutive Patients with Intracranial Hemorrhage

Patient no.	Age (y)	Sex	Location	Timing (d)	Visual analysis	MIBI index	Timing (d)	Visual analysis	MIBI index
1	78	F	Left parietal	2	Negative	1.01	30	Positive	2
2	37	F	Right temporal	2	Negative	1.02	30	Positive	1.9
3	60	M	Left parietal	2	Negative	0.97	30	Positive	2.1
4	80	F	Left occipital	2	Negative	1.1	30	Positive	1.8
5	76	F	Left frontal	2	Negative	1	30	Positive	2
6	67	F	Right parietal	2	Negative	1.08	30	Positive	1.7
7	73	M	Right temporal	2	Negative	0.95	30	Positive	1.8
8	69	M	Left parietal	2	Negative	1.09	30	Positive	1.7
9	77	F	Right temporal	5	Positive	1.7			
10	63	F	Right frontal	5	Negative	1.08			
11	73	F	Right temporal	5	Negative	1.2			
12	65	M	Left parietal	5	Negative	1			
13	49	M	Right frontal	5	Negative	0.98			
14	63	M	Left frontal	5	Negative	0.96			
15	65	M	Right temporal	5	Negative	1.03			
16*	64	F	Left parietal	5	Positive	2.2			
17	55	M	Right parietal	10	Positive	1.33			
18	78	F	Left parietal	10	Positive	1.4			
19	71	M	Right frontal	10	Positive	1.9			
20	81	M	Right temporal	10	Positive	1.8			
21	76	F	Left temporal	10	Positive	1.6			
22	69	M	Right temporal	10	Negative	1.09			
23	65	M	Left temporal	10	Negative	1			
24	64	F	Left frontal	10	Negative	1.03			
25	62	M	Right parietal	30	Positive	2			
26	66	M	Left parietal	30	Positive	2.3			
27	68	F	Left temporal	30	Positive	1.7			
28	71	M	Right occipital	30	Positive	1.5			
29	69	F	Left frontal	30	Positive	1.8			
30*	70	M	Right parietal	30	Positive	2.8			
31	61	M	Cerebellar	30	Negative	1.1			
32	71	M	Mesencephalus	30	Negative	1.08			

*Patient with neoplastic hemorrhage.

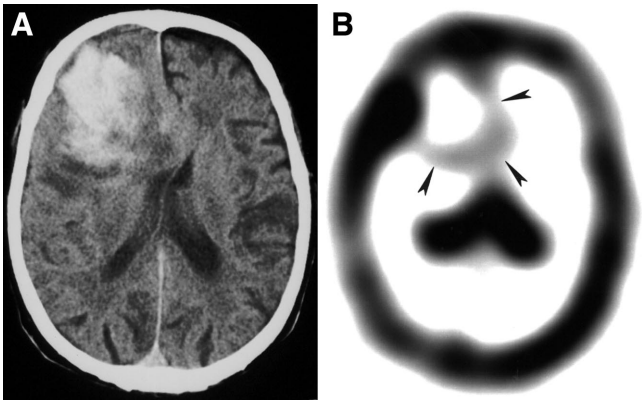

FIGURE 1. Patient 19, a 71-y-old man with sudden onset of left-sided hemiparesis and drowsiness. (A) Emergency CT scan shows atypically located 5-cm large, inhomogeneous hematoma in right frontal region. Lesion is surrounded by moderate edema and determines compression of lateral ventricles and subfalcine herniation. (B) ^{99m}Tc-MIBI SPECT image obtained at 10 d shows ringlike ^{99m}Tc-MIBI uptake at periphery of lesion (arrowheads) (^{99m}Tc-MIBI index = 1.9).

SPECT Data Analysis

^{99m}Tc-MIBI SPECT studies were visually and semiquantitatively evaluated by 2 independent nuclear medicine physicians (1 more experienced and 1 less experienced) who were aware of the emergency CT results but not of the other clinical and neuroradiologic data.

For the visual analysis, findings were considered negative when activity was absent or faintly increased, compared with the contralateral side, and positive when activity was clearly increased.

For the semiquantitative analysis, after spatial localization of the lesion using CT as a guide, a round region of interest (ROI) was drawn encompassing the area of maximal uptake near the lesion. During this procedure, images were displayed with the base and window settings held constant. ^{99m}Tc-MIBI index was obtained as the ratio of average counts in the lesion ROI to the average counts in its contralateral homologous mirror image. If the control ROI was close to the scalp or choroid plexus or if the lesion was on the midline, the control ROI was drawn on an uninvolved area of cerebral parenchyma.

Statistical Analysis

Statistical analysis was based on data provided by the first observer. In addition, data determined by the 2 observers were evaluated for interobserver agreement; interobserver variability was measured using the weighted κ statistic. Tracer uptake was compared among the 4 groups using the Fisher exact test for the visual analysis and using ANOVA with the Tukey test for the semiquantitative analysis. Finally, the paired *t* test was used to assess the difference in tracer uptake between the first and second examinations for patients who underwent repeated ^{99m}Tc-MIBI SPECT. Computation was supported by the statistical packages InStat 3.0 and Prism 4.0 (GraphPad Software) and MedCalc 7.2.1.0 (MedCalc Software) for Windows (Microsoft). A P value of 0.05 was used to define statistical significance.

RESULTS

Thirty-two patients (18 men and 14 women; mean age, 67 y; range, 37–81 y) were enrolled in the study. Patients 16 and 30, who underwent ^{99m}Tc-MIBI SPECT at 5 d (group 2) and 30 d (group 4), respectively, after symptom onset, were excluded from the analysis because neoplastic ICH was diagnosed. The diagnosis of neoplastic ICH was suggested by neuroimaging and was confirmed by open surgery (bleeding metastasis from malignant melanoma and hemorrhagic glioblastoma multiforme). Both these patients had positive SPECT findings, with a 2.2 and 2.8 ^{99m}Tc-MIBI index, respectively.

Accordingly, 30 patients with a final diagnosis of nonneoplastic ICH were considered for statistical evaluation. Visual analysis showed no focal increased tracer uptake (0% positive findings) in group 1 (day 2). In group 2 (day 5), visual analysis showed increased tracer uptake in 1 of 7 patients (14% positive findings). In group 3 (day 10), visual analysis showed increased tracer uptake in 5 of 8 patients (62.5% positive findings) (Figs. 1 and 2). In group 4 (day 30), visual analysis showed increased tracer uptake in 5 of 7 patients (71% positive findings).

Visual analysis showed no significant difference in tracer uptake between groups 1 and 2 or between groups 3 and 4, whereas a statistically significant difference was found between groups 1 and 3 ($P = 0.02$), groups 1 and 4 ($P = 0.001$), and groups 2 and 4 ($P = 0.03$) (Fig. 3). We also compared patients studied within 5 d (groups 1 and 2) with patients studied 10 and 30 d after clinical onset (groups 3 and 4, respectively), and we found a statistically significant difference ($P = 0.008$ and $P = 0.004$, respectively).

In the semiquantitative analysis, the ^{99m}Tc-MIBI index for nonneoplastic ICH ranged from 0.95 to 1.1 (mean, 1.03 ± 0.06) in group 1, from 0.96 to 1.7 (mean, 1.14 ± 0.26) in group 2, from 1 to 1.9 (mean, 1.39 ± 0.35) in group 3, and from 1.08 to 2.3 (mean, 1.64 ± 0.45) in group 4. Even using ^{99m}Tc-MIBI index values, we found a statistically significant difference between groups 1 and 3 ($P = 0.01$), groups 1 and 4 ($P = 0.002$), and groups 2 and 4 ($P =$

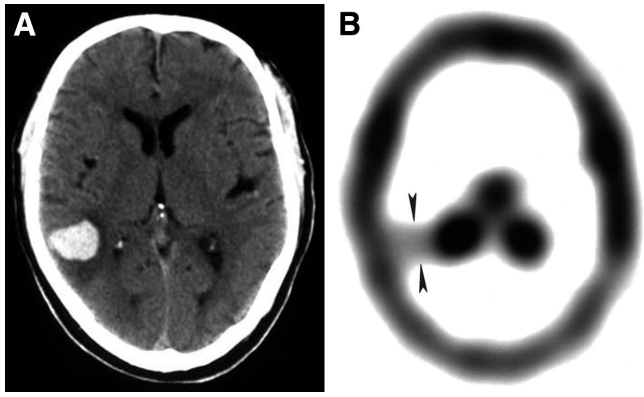

FIGURE 2. Patient 17, a 55-y-old man with sudden onset of cephalalgia. (A) Emergency CT scan shows atypically located 25-mm large, round hematoma in right paratrigonal region. Lesion is surrounded by moderate edema. (B) ^{99m}Tc-MIBI SPECT image obtained at 10 d shows homogeneous focal area of ^{99m}Tc-MIBI uptake (arrowheads) (^{99m}Tc-MIBI index = 1.33).

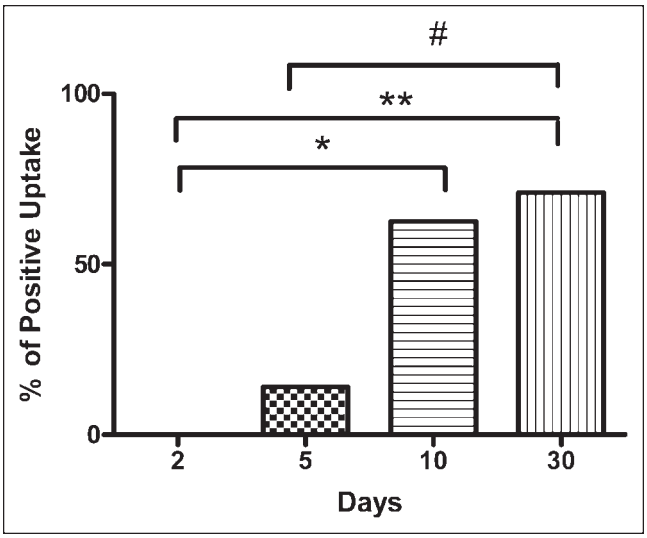

FIGURE 3. Bar graph showing ^{99m}Tc-MIBI uptake in 4 groups of patients who underwent ^{99m}Tc-MIBI SPECT 2, 5, 10, and 30 d after onset of clinical deterioration. Statistically significant difference was found between groups 1 and 3 (*P = 0.02), groups 1 and 4 (**P = 0.001), and groups 2 and 4 (#P = 0.03).

0.02). We also compared patients studied within 5 d (groups 1 and 2) with patients studied 10 and 30 d after clinical onset (groups 3 and 4, respectively), and we found a statistically significant difference (P = 0.009 and $P < 0.001$, respectively).

All patients in group 1, who showed no focal increased radiotracer uptake at 2 d after the onset of clinical symptoms, showed significant ^{99m}Tc-MIBI accumulation when studied at 30 d after the onset (mean ^{99m}Tc-MIBI index, 1.88 ± 0.15; range, 1.7–2.1) (Fig. 4). The difference was statistically significant ($P < 0.001$).

Finally, agreement between the 2 observers was complete for the visual analysis and excellent for the ^{99m}Tc-MIBI index (κ = 0.98; SE = 0.16).

DISCUSSION

Distinguishing between hemorrhagic intracranial neoplasms and nonneoplastic hematomas is often difficult because of the considerable overlap between their neuroradiologic imaging findings (*13–18*). Furthermore, because the neuroradiologic diagnosis of neoplasm-related hemorrhage is frequently based on evolution patterns (*13,14*), a complex diagnostic protocol is frequently needed and diagnosis can be delayed significantly.

In a recent paper (*7*), ^{99m}Tc-MIBI SPECT was proposed as a useful tool in the early differential diagnosis of ICH. The differential diagnosis was based on the presence of ^{99m}Tc-MIBI uptake in neoplastic ICH and the lack of radiotracer accumulation in nonneoplastic ICH. All the cases of ICH in that study were evaluated within 48 h from the onset of clinical symptoms, and ^{99m}Tc-MIBI SPECT turned out to be 100% sensitive and specific.

The lack of metabolically active cells, whose presence seems strongly related to ^{99m}Tc-MIBI retention (*19–22*), was considered responsible for the absence of ^{99m}Tc-MIBI accumulation in early-phase nonneoplastic hematomas.

However, the neuropathologic features of ICH significantly change over time with the proliferation of many metabolically active cells, mainly at the periphery of the lesion (*8–12*). Enzmann et al. (*8*), who studied the evolution of intracerebral hemorrhage using a canine model, categorized the evolution of intracerebral hemorrhage into 4 stages: acute, subacute, capsule, and organization. In the acute stage (days 1–3), only mild perivascular inflammatory reaction and a narrow zone of neuron death may occur. In the subacute stage (days 4–8), inflammation peaks, foamy macrophages and fibroblasts appear peripherally, and reactive astrocytes appear in the surrounding brain. During the capsule stage (days 9–13), macrophages and fibroblasts increase and vascular proliferation begins to encroach on the hematoma from the periphery. At the same time, inflammation regresses and reactive astrocytosis becomes pronounced. The formation of a dense capsule at the edge of the hematoma and a less organized collagen proliferation in the center of the hematoma occurs in the organization stage (days 13 and on).

Our study demonstrated that nonneoplastic brain hematoma may show radiotracer accumulation on ^{99m}Tc-MIBI SPECT and that, because of the neuropathologic changes that occur over time, the appearance is related to the timing of the examination. This concept is particularly supported by our results for the patients who underwent 2 different SPECT examinations—at 2 d and at 30 d—because no

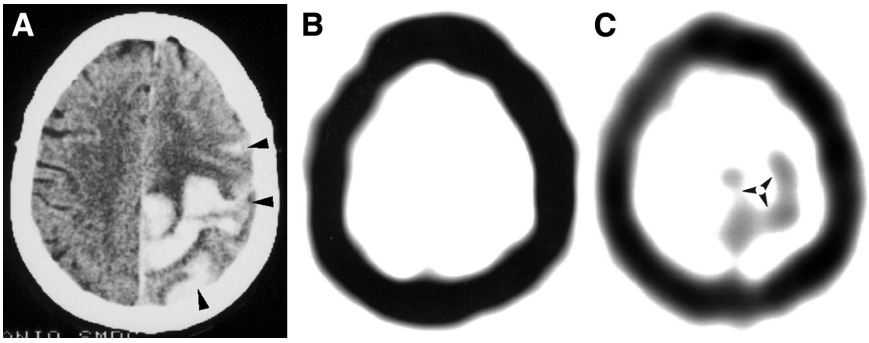

FIGURE 4. Patient 5, a 76-y-old woman with sudden onset of aphasia, right-sided hemiparesis, and drowsiness. (A) Emergency CT scan shows atypically located hematoma in left frontal region with subarachnoid spreading (arrowheads). Lesion is surrounded by moderate edema. (B) ^{99m}Tc-MIBI SPECT image obtained 2 d after onset of clinical deterioration shows no ^{99m}Tc-MIBI uptake (^{99m}Tc-MIBI index = 1). (C) ^{99m}Tc-MIBI SPECT image obtained 30 d after onset of clinical deterioration shows ringlike ^{99m}Tc-MIBI uptake (arrowheads) (^{99m}Tc-MIBI index = 2).

reasonable hypothesis other than the timing of the examination could explain the difference in the appearance of nonneoplastic ICH in these 2 examinations (Fig. 4).

Although ^{99m}Tc-MIBI uptake has never, to our knowledge, been reported in patients with nonneoplastic brain hematomas (*22*), radiotracer accumulation has been described in patients with ICH studied by ^{201}Tl SPECT (*23–25*), ^{18}F-FDG PET, and ^{11}C-methionine PET (*26–28*). Interestingly, in 7 cases of nonneoplastic hematoma evaluated by ^{11}C-methionine PET in 2 different studies (*26,27*), uptake occurred in 6 patients studied 20–45 d after the bleeding, whereas no ^{11}C-methionine accumulation occurred in a cerebellar hematoma studied only 5 d after the bleeding. Furthermore, of 6 patients with intracranial hemorrhage studied by ^{201}Tl SPECT 9–39 d after the bleeding, 1 showed focal radiotracer accumulation (*25*).

In the present study, we found ^{99m}Tc-MIBI accumulation on delayed examinations. Particularly, we found a statistically significant difference in tracer uptake between patients studied within 5 d after symptom onset (groups 1 and 2) and patients studied at 10 and 30 d (groups 3 and 4, respectively) after symptom onset.

^{99m}Tc-MIBI accumulation was detected in all but 2 patients studied 30 d after symptom onset. Noteworthy, the ICH of those 2 patients was in the posterior fossa. This different location of the ICH may have been responsible for its different appearance on ^{99m}Tc-MIBI SPECT (*29*).

On ^{99m}Tc-MIBI SPECT examinations with positive findings, most nonneoplastic hematomas showed a ringlike pattern of accumulation (Figs. 1B and 4C). This pattern could be explained by peripheral accumulation of metabolically active cells. Ringlike radiotracer accumulation in brain hematomas is not completely surprising, because it has previously been reported in a few patients imaged with ^{201}Tl (*24*) or ^{11}C-methionine (*26,27*) and is similar to the ring enhancement that can be seen on CT scans (*8–11,30*). A ringlike pattern of ^{99m}Tc-MIBI accumulation is not specific to nonneoplastic ICH; other pathologic entities such as metastases and high-grade gliomas may have a similar appearance (*22*). However, additional studies are needed to verify whether a differential diagnosis may be obtained by means of ^{99m}Tc-MIBI indices.

This study demonstrated that the reliability of ^{99m}Tc-MIBI SPECT in revealing neoplastic ICH significantly decreased as the time between bleeding and examination increased. No patients with nonneoplastic ICH in this study showed ^{99m}Tc-MIBI accumulation at 2 d, whereas 14% of patients studied at 5 d, 62.5% of patients studied at 10 d, and 71% of patients studied at 30 d showed radiotracer uptake.

Our study suffered from some limitations. One limitation could be the small number of patients who underwent repeated ^{99m}Tc-MIBI SPECT examinations at different times. However, certain ethical considerations discourage performing multiple SPECT examinations on the same patient, and we believe that our goal (i.e., to demonstrate a difference in appearance for nonneoplastic hematomas on early and delayed ^{99m}Tc-MIBI SPECT images) was nevertheless achieved.

Another limitation could be the lack of histopathologic specimens for correlation of imaging findings with pathologic findings. This limitation could not be obviated, because biopsies cannot be performed in the clinical setting of intracerebral nonneoplastic hematomas. However, the previous studies on the neuropathology of intracranial hemorrhage (*8–12*) permit us to reliably hypothesize the pathologic abnormalities that may correlate with and explain the imaging findings.

CONCLUSION

Nonneoplastic ICH, showing no ^{99m}Tc-MIBI uptake within 2 d, can accumulate ^{99m}Tc-MIBI on more delayed imaging. ^{99m}Tc-MIBI SPECT can clearly differentiate between neoplastic and nonneoplastic ICH only in the acute phase. Our findings suggest that the examination should be performed early after symptom onset and certainly within 5 d.

ACKNOWLEDGMENTS

This study was supported in part by grant FIRB 2001 from Ministero dell'Istruzione, dell'Università e della Ricerca, protocol no. RBNE01MBEC.

REFERENCES

1. Schrader B, Barth H, Lang EW, et al. Spontaneous intracranial haematomas caused by neoplasms. *Acta Neurochir.* 2000;142:979–985.
2. Wakai S, Yamakawa S, Manaka S, Takakura K. Spontaneous intracranial haemorrhage caused by brain tumour: its incidence and clinical significance. *Neurosurgery.* 1982;10:437–444.
3. Maiuri F, D'Andrea F, Gallicchio B, Carandente M. Intracranial haemorrhages in metastatic brain tumours. *J Neurosurg Sci.* 1985;29:37–41.
4. Iwama T, Ohkuma A, Miwa Y, et al. Brain tumours manifesting as intracranial haemorrhage. *Neurol Med Chir.* 1992;32:130–135.
5. d'Avella D, Germanò A, Romano A, Cardia E, Tomasello F. Chronic encapsulated intracerebral hematoma: contribution of thallium-201 single photon emission computed tomography in preoperative diagnosis: case report. *Neurosurgery.* 1997;41:677–679.
6. Kuhner A, Scheidet D. Pseudotumour forms of spontaneous intracerebral haematomas. *Neurochirurgia.* 1988;31:118–122.
7. Minutoli F, Angileri FF, Cosentino S, et al. ^{99m}Tc-MIBI SPECT in distinguishing neoplastic from nonneoplastic intracerebral hematoma. *J Nucl Med.* 2003;44:1566–1573.
8. Enzmann DR, Britt RH, Lyons BE, Buxton JL, Wilson DA. Natural history of experimental intracerebral hemorrhage: sonography, computed tomography and neuropathology. *Am J Neuroradiol.* 1981;2:517–526.
9. Lee YY, Moser R, Bruner JM, Van Tassel P. Organized intracerebral hematoma with acute hemorrhage: CT patterns and pathologic correlations. *AJR.* 1986;147:111–118.
10. Laster DW, Moody DM, Ball MR. Resolving intracerebral hematoma: alteration of the "ring sign" with steroids. *AJR.* 1978;130:935–939.
11. Takasugi S, Ueda S, Matsumoto K. Chronological changes in spontaneous intracerebral hematoma: an experimental and clinical study. *Stroke.* 1985;16:651–658.
12. Andaluz N, Zuccarello M, Wagner KR. Experimental animal models of intracerebral hemorrhage. *Neurosurg Clin North Am.* 2002;13:385–393.
13. Atlas S, Grossman R, Gomori JM, et al. Hemorrhagic intracranial malignant neoplasm: spin-echo MR imaging. *Radiology.* 1987;164:71–77.
14. Destian S, Sze G, Krol G, Zimmerman RD, Deck MD. MR imaging of hemorrhagic intracranial neoplasm. *AJR.* 1989;152:137–144.
15. Gaul HP, Wallace CJ, Crawley AP. Reverse enhancement of hemorrhagic brain

lesions on postcontrast MR: detection with digital image subtraction. *Am J Neuroradiol.* 1996;17:1675–1680.
16. Chan JH, Peh WC. Methemoglobin suppression in T2-weighted pulse sequences: an adjunctive technique in MR imaging of hemorrhagic tumors. *AJR.* 1999;173: 13–14.
17. Hanna SL, Langston JW, Gronemeyer SA. Value of subtraction images in the detection of hemorrhagic brain lesions on contrast-enhanced MR images. *Am J Neuroradiol.* 1991;12:681–685.
18. Parizel PM, Makkat S, Van Miert E, Van Goethem JW, van Den Hauwe L, De Schepper AM. Intracranial hemorrhage: principles of CT and MRI interpretation. *Eur Radiol.* 2001;11:1770–1783.
19. Chiu M, Kronauge JF, Piwnica-Worms D. Effect of mitochondrial and plasma membrane potentials on accumulation of hexakis (2 methoxyisobutylisonitrile) technetium (I) in cultured mouse fibroblasts. *J Nucl Med.* 1990;31:1646–1653.
20. Crane P, Laliberte R, Heminway S. Effect of mitochondrial viability and metabolism of technetium-99m-sestamibi. *Eur J Nucl Med.* 1993;20:20–25.
21. Savi A, Gerundini P, Zoli P, et al. Biodistribution of Tc-99m-methoxy-isobutyl-isonitrile (MIBI) in humans. *Eur J Nucl Med.* 1989;15:597–600.
22. Baldari S, Restifo Pecorella G, Cosentino S, Minutoli F. Investigation of brain tumors with ^{99m}Tc-MIBI SPET. *Q J Nucl Med.* 2002;46:336–345.
23. Sun D, Liu Q, Liu W, Hu W. Clinical application of ^{201}Tl SPECT imaging of brain tumors. *J Nucl Med.* 2002;41:5–10.
24. Kinuya K, Ohashi M, Itoh S, et al. Differential diagnosis in patients with ring-like thallium-201 uptake in brain SPECT. *Ann Nucl Med.* 2002;16:417–421.
25. Dierckx RA, Martin JJ, Dobbeleir A, Crols R, Neetens I, De Deyn PP. Sensitivity and specificity of thallium-201-single-photon emission tomography in the functional detection and differential diagnosis of brain tumours. *Eur J Nucl Med.* 1994;21:621–633.
26. Dethy S, Goldman S, Blecic S, Luxen A, Levivier M, Hildebrand J. Carbon-11-methionine and fluorine-18-FDG PET study in brain hematoma. *J Nucl Med.* 1994;35:1162–1166.
27. Ogawa T, Hatazawa J, Inugami A, et al. Carbon-11-methionine PET evaluation of intracerebral hematoma: distinguishing neoplastic from non-neoplastic hematoma. *J Nucl Med.* 1995;36:2175–2179.
28. Nakagawa M, Kuwabara Y, Sasaki M, et al. ^{11}C-methionine uptake in cerebrovascular disease: a comparison with ^{18}F-fDG PET and ^{99m}Tc-HMPAO SPECT. *Ann Nucl Med.* 2002;16:207–211.
29. Bagni B, Pinna L, Tamarozzi R, et al. SPET imaging of intracranial tumours with ^{99m}Tc-sestamibi. *Nucl Med Commun.* 1995;16:258–264.
30. Zimmerman RD, Leeds NE, Naidich TP. Ring blush associated with intracerebral hematoma. *Radiology.* 1977;122:707–711.